Nuclear Reactions in Stars. IV. Buildup from Carbon*

H. REEVES† AND E. E. SALPETER
Laboratory of Nuclear Studies, Cornell University, Ithaca, New York
(Received June 1, 1959)

Reaction leading to the formation of C, O, and Ne at temperatures T of about 10^8 °K, in the core of red giant stars, had been studied previously. The nuclear reactions and resulting nucleogenesis are now studied for a gas consisting of C^{12}, O^{16}, and Ne^{20} at 6×10^8 to 10×10^8 °K and densities around 10^4 g/cc. The basic reaction rates are calculated and a set of simultaneous differential equations for various abundances as a function of time is solved numerically.

The C^{12} is destroyed by compound nucleus formation from C+C collisions in about 10^5 and 1 years, respectively, at 6×10^8 and 8.5×10^8 °K. The net result is the production of some additional amounts of O^{16} and Ne^{20}; appreciable amounts of Na^{23} and the three stable magnesium isotopes (mainly Mg^{24}) and decreasing amounts of Al^{27}, Si, etc. The ratio of Na^{23} to Mg^{24} produced is almost $\frac{1}{2}$, appreciably larger than the "cosmic" ratio.

During the carbon burning, protons and alphas are released. At temperatures below 7×10^8 °K, neutrons are produced very copiously through the sequence $C^{12}(p,\gamma)N^{13}$; $N^{13}\rightarrow C^{13}$; $C^{13}(\alpha,n)O^{16}$. If small amounts of metals in the Fe-region (up to about one metal nucleus per 1000 C^{12} nuclei) were present originally, each metal nucleus will absorb about 30 neutrons. At temperatures above 8×10^8 °K, N^{13} is photodisintegrated and the neutron production is appreciably less.

1. INTRODUCTION

THIS paper is a continuation of a series entitled "Nuclear Reactions in Stars." The first three papers,[1–3] hereafter referred to as I, II, III, followed the history of a hypothetical star (originally consisting of pure hydrogen) up to the point where its core, composed mainly of helium, carbon, oxygen, and neon, is the seat of reactions of the (α,γ) type, by which the helium concentration is slowly being exhausted. At least for stars of about 1.5 solar mass, the evolutionary stage at which this helium burning takes place is reasonably well known—the "tip of the red giant branch"—and the situation is probably rather similar for more massive stars. In the cores of these stars, the helium is effectively processed at temperatures of about 1.5×10^8 °K. The main constituents are then C^{12}, O^{16}, and Ne^{20}, but the relative abundances of these three species are somewhat uncertain and depend on the temperature and density at which the hydrogen burning takes place.

Unless the densities become extremely high, the temperature has to be raised by a considerable factor—about 5—before any further nuclear reactions can proceed at an appreciable rate. The first such reaction to take place involves the collision between two C^{12} nuclei. The main object of the present paper is to analyze the nuclear aspects of this reaction.[4,5] The C−C collisions release α particles and protons which can take part in a complicated network of reactions, including the production and absorption of neutrons. The details of these reactions depend on the time scale of the original C−C reactions (controlled by the temperature), especially on whether the reaction times are long or short compared with beta-decay times. There probably exists a wide variety of stars in which temperatures are high enough for C−C reactions to proceed, although at the moment we have no direct astrophysical information on any of them. In supernovae, the time scale of the reactions is likely to be very short. We shall not discuss such cases, but restrict ourselves to reaction times of about 1 to 10^6 years, all long compared with most beta-decay times. The corresponding range of temperatures is about 6×10^8 to 9×10^8 °K.

In Sec. 2, we summarize the approximations and techniques used in evaluating rates for various capture and photodisintegration reactions. In Sec. 3, we calculate rates for the key reaction involving the collision of two C^{12} nuclei which can result in $Ne^{20}+\alpha$, $Na^{23}+p$, $Mg^{23}+n$, or $Mg^{24}+\gamma$. The rates at which the α, p, n thereby produced will react with the constituents of the stellar gas is discussed in Sec. 4, and the variation with time of isotopic abundances, caused by this network of reactions, in Sec. 5. During the course of these reactions, neutrons are produced rather copiously, and we also discuss in these sections the buildup of heavy elements by neutron absorption if some metals were present in the original gas.

In Sec. 6 we consider briefly the sequence of events in the stellar core, if the temperature keeps on increasing slowly. In Sec. 7 we compare the isotopic abundances at the end of the carbon burning with the cosmic abundances, and we draw some tentative conclusions of astrophysical interest.

2a. REACTIONS INVOLVING CHARGED PARTICLES

The formalism for computation of reaction rates involving protons and alphas has been developed in I, II, and III. We shall use it here with the same

* Supported in part by the joint program of the Office of Naval Research and the U. S. Atomic Energy Commission.
† Now at Physics Department, Université de Montreal, Montreal, Canada.
[1] E. E. Salpeter, Phys. Rev. **88**, 547 (1952).
[2] E. E. Salpeter, Phys. Rev. **97**, 1237 (1955).
[3] E. E. Salpeter, Phys. Rev. **107**, 547 (1957).
[4] A preliminary report of this work has been given by H. Reeves and E. E. Salpeter, Bull. Am. Phys. Soc. Ser. II, **3**, 227 (1958).
[5] Similar work, from slightly different points of view, has been done by: C. Hayashi *et al.*, Progr. Theoret. Phys. (Kyoto) **20**, 110 (1958); A. G. W. Cameron, Astrophys. J. (to be published).

notation.[6] However, because of the somewhat higher temperatures involved in this work, it will be necessary to introduce some modifications, as follows:

The first type of modification concerns the computation of Coulomb barrier penetration probability. In the series expansion of G_l^{-2}, the irregular Coulomb[7] wave function for charged particles evaluated at a nuclear interaction radius R we shall need to keep one more term in the exponent than in I, II, and III, namely:

$$\begin{aligned} G_0^{-2} &= 2(\eta/y^{\frac{1}{2}})\exp[4y^{\frac{1}{2}}-2\pi\eta-y^{\frac{3}{2}}/6\eta^2], \\ 4y^{\frac{1}{2}} &= 1.054[Z_1Z_2MR]^{\frac{1}{2}}, \\ 2\pi\eta &= 0.989[Z_1^2Z_2^2M/E]^{\frac{1}{2}}, \\ y^{\frac{3}{2}}/6\eta^2 &= 0.122[MR^3E^2/Z_1Z_2]^{\frac{1}{2}}; \end{aligned} \tag{1}$$

M is the reduced mass.

We obtain the G_l^{-2} for nonzero values of the orbital quantum number with the help of the recursion relations given in the same reference. To take into account the effect of these modifications in the rates, we shall redefine (and prime) some of the expressions used previously. First, we want to extract from some of the "constants" the energy dependence afflicted on them by the higher temperature involved. We define

$$\xi_l'^2 = \xi_l^2 \exp(y^{\frac{3}{2}}/6\eta^2) = (G_0^2/G_l^2)(2y^{\frac{1}{2}})\exp(4y^{\frac{1}{2}}), \tag{2}$$

$$S' = S\exp(y^{\frac{3}{2}}/6\eta^2) = \sigma E\exp(2\pi\eta+y^{\frac{3}{2}}/6\eta^2). \tag{3}$$

Then $\xi_l'^2$ and S' are almost energy-independent, and we have

$$\Gamma_c = \gamma^*\exp(-2\pi\eta-y^{\frac{3}{2}}/6\eta^2)\xi_l'^2, \tag{4}$$

where Γ_c is the width for a charged particle and $\gamma^*\equiv\gamma^2/R$ is the reduced width in energy units.

Such changes will effect the resonant rate only through the reduction to Γ_c in Eq. (4), compared with the approximation used in reference 3. On the nonresonant rate, they are tantamount to a rescaling of the temperature; the modified rate at T equals the nonmodified rate at an effective temperature T' defined by

$$T' = T(1-\epsilon)\equiv T[1-10^{-3}(MR^3T^2/Z_1Z_2)^{\frac{1}{2}}], \tag{5}$$

where ϵ is defined by Eq. (5). Consequently the Gamow peak E_m (the energy from which the contribution to the nonresonant rate is a maximum) will be shifted towards the origin:

$$\begin{aligned} E_m' &= E_m(1-2\epsilon/3) \\ &= 2.63\times10^{-2}(Z_1^2Z_2^2MT^2)^{\frac{1}{3}}(1-2\epsilon/3), \end{aligned} \tag{6}$$

and its full width at half-maximum, Γ_m, becomes

$$\Gamma_m' = 2.88\times10^{-2}(T^5Z_1^2Z_2^2M)^{1/6}(1-5\epsilon/6). \tag{7}$$

Finally, the exponent τ is transformed into

$$\tau' = 9.152(Z_1^2Z_2^2M/T)^{\frac{1}{3}}(1+\epsilon/3), \tag{8}$$

and the nonresonant rate $p_{\text{n.r.}}$ is

$$\begin{aligned} p_{\text{n.r.}} &= [\rho x_1/A_1](1/MZ_1Z_2) \\ &\quad\times\tau'^2(e^{-\tau'})434\times10^6S' \quad (\text{sec}^{-1}). \end{aligned} \tag{9}$$

We recall that p^{-1} is the mean lifetime of a nucleus of species 2 in a gas of density ρ, fractional density x_1 of particles of species 1 (by mass). S' is in Mev barns, in the center-of-mass system.

We shall find it useful to use the reaction probability per pair of particles $\mathcal{P}$:

$$\mathcal{P} = (p/\mathfrak{N})(A_1/\rho x_1) \tag{10}$$

($\mathfrak{N}$ is Avogadro's number), and to express these rates under the form of logarithm to the base 10:

$$\begin{aligned} \log_{10}\mathcal{P}_{\text{n.r.}} &= -15.14-\log(MZ_1Z_2)+\log S' \\ &\quad+2\log\tau'-0.434\tau'. \end{aligned} \tag{11}$$

To give an idea of the magnitude of these corrections, we take for example, the case of the carbon-carbon collision at $T=6\times10^8$ °K. In this case the Gamow peak is reduced from 1.7 Mev to 1.6 Mev, and the reaction rate is reduced by a factor of 7.

The second kind of revision needed here involves the nuclear part of the reaction. Cases for which the Breit-Wigner single-level formula for the cross section is a good approximation are treated as in III with appropriate modifications. The factor $S_{\text{B.W.}}'$ becomes

$$\begin{aligned} S_{\text{B.W.}}' &= (0.647/M)\xi_l'^2 \\ &\quad\times(\omega\gamma^*\Gamma_{\text{out}}/[(E_m'-E_r)^2+\Gamma^2/4]). \end{aligned} \tag{12}$$

Here ω is a statistical factor: $\omega=(2j_{\text{C.N.}}+1)/(2j_1+1)(2j_2+1)$; j_1 is the spin of particle 1, j_2 is the spin of particle 2, $j_{\text{C.N.}}$ is the spin of the state of the compound nucleus formed in the process. Γ_{out} is the partial width of the exit channel, and E_r is the resonant energy.

The nonresonant rate is found by substitution of Eq. (12) in Eq. (11). The resonant rate is given by

$$\begin{aligned} \log\mathcal{P}_r &= -11.09+\log\omega(\Gamma_C\Gamma_{\text{out}}/\Gamma) \\ &\quad-\tfrac{3}{2}\log M-\tfrac{3}{2}\log T-50.4E_r/T. \end{aligned} \tag{13}$$

When many resonances are expected to be found within the Gamow peak, but little is known about their individual characteristics, the following approximation becomes useful: We assume that at every temperature considered, there is a resonance exactly in the center of the Gamow peak. We compute the corresponding rate and multiply by the number of resonances to be found within the Gamow width. This prescription overestimates the rate only slightly.

Finally, in some of the cases considered here, it will be convenient to abandon the Breit-Wigner approximation to the cross section, and to go to the other

[6] All through the present work, unless otherwise noted, energies (resonances, widths, etc.) will be in units of Mev; temperatures in 10^8 °K; radii in fermis [1 fermi (f) $\equiv10^{-13}$ cm], cross sections in barns, reaction probabilities in sec^{-1}; masses in atomic mass units. We are always in the center-of-mass system.

[7] H. Feshbach *et al.*, Atomic Energy Commission Report NYO-3077 (unpublished).

extreme, namely to the picture of the nucleus as "black." We shall use this picture especially for the C−C reaction. Such a picture assumes that so many channels are open for the compound nucleus to decay that the chances for an exit through the entrance channel are negligible. This is represented in the formalism by taking the logarithmic derivative of the wave function as being purely imaginary at the surface of the nucleus.

The reaction cross section $\sigma_l(E)$ for an incident particle of relative energy E, angular momentum l is then given by

$$\sigma_l(E)=\omega\pi\lambda\!\!\!^{-2}T_l(E). \tag{14}$$

In the energy range considered here $T_l(E)$, the transmission coefficient, can be written as:

$$T_l(E)=4(k/K)G_l^{-2}. \tag{15}$$

Here, k is the wave number far away from the nucleus, and K is an average wave number inside the nucleus ($K\sim 1$ f^{-1}).

If the nucleus is fully "black" an incident particle with any energy and angular momentum can find an open channel to penetrate the nucleus. In this case, we compute the rate contributed by each partial wave and sum over all partial waves. If the levels of the compound nucleus do not overlap completely we get a simple approximation by multiplying the "black-nucleus" rate by n, the ratio of the average level width to the average spacing between levels of the same spin and parity. For collisions between two spinless nuclei only levels of the type 0^+, 1^-, 2^+, 3^-, etc. (which we shall call "active" levels) contribute.

Our "black-nucleus" approximation for the cross-section factor S_b' is then:

$$S_b'=0.70(Z_1Z_2/MR)^{\frac{1}{2}}Hn\exp(4y^{\frac{1}{2}}),$$
$$H=\sum_{l=0}^{\infty}(2l+1)G_0^2/G_l^2. \tag{16}$$

The reaction rate is found by substituting Eq. (16) into Eq. (11).

2b. REACTIONS INVOLVING NEUTRONS

We can again break the reaction rate into a resonant and a nonresonant contribution. For $l=0$ neutrons, the nonresonant rate is likely to be important because of the well-known $(1/v)$ behavior of the cross section at low energy. Then

$$\mathcal{P}_{\text{n.r.}}=\sigma v=\text{constant}. \tag{17}$$

This is valid for all energies where the $1/v$ law holds. It is enough to know the cross section $\sigma(E)$ at any one energy (E) to obtain $\mathcal{P}_{\text{n.r.}}$:

$$\mathcal{P}_{\text{n.r.}}=1.39\times 10^{-15}\sigma(E)(E^{\frac{1}{2}}/M^{\frac{1}{2}}),$$
$$\sigma \text{ in barns, } E \text{ in Mev}. \tag{18}$$

If the thermal cross section is known,

$$\mathcal{P}_{\text{n.r.}}=2.17\times 10^{-19}(\sigma_{\text{th}}/M^{\frac{1}{2}}). \tag{19}$$

Even a smooth departure from the $1/v$ law can be handled this way by a proper adjustment of the computed rate.[8]

If a resonance occurs at an energy $E\leqslant 10kT$, then the resonant rate may be more important. In such a case, we use Eq. (13), taking the neutron width as the incident width.

The temperature dependence of neutron capture rates is far less important than the temperature of charged particle rates.

2c. PHOTODISINTEGRATION RATES

The probability $\mathcal{P}^{\text{dis}}$ that an excited nucleus will be photodisintegrated can be equated to the relative probability $p(E^*)$ that the nucleus will be found excited at an energy E^*, times the probability $\Gamma_{\text{dis}}(E^*)/\hbar$ that the nucleus will be photodisintegrated, given that it has an excitation energy E^*.

If the nucleus has an excited state at E^*, above but close to the separation energy of the constituent parts, most of the photodisintegration rate will be contributed by this state. In a gas in thermal equilibrium with its radiation, $p(E^*)$ is then the product of a statistical factor, times a Maxwellian factor, times a factor which takes into account the relative depopulation of that state due to the possibility of photodisintegration:

$$p(E^*)=[(2J+1)/(2I+1)][\exp(-E^*/kT)]\times\{\Gamma_\gamma/[\Gamma_\gamma+\Gamma_{\text{dis}}(E_r)]\}, \tag{20}$$

E_r is the energy gap between the resonance E^* and the separation energy Q, J and I are, respectively, the spins of the excited state and of the ground state. $\Gamma_\gamma(E_r)$ is the probability of de-excitation through gamma emission, and $\Gamma_{\text{dis}}(E_r)$ is the probability of photodisintegration. We recall that $\Gamma_{\text{dis}}(E_r)$ is identical with $\Gamma_C(E_r)$, the partial width for capture of these constituents.

The resonant photodisintegration rate $\mathcal{P}_r^{\text{dis}}$ becomes

$$\log\mathcal{P}_r^{\text{dis}}=21.15+\log\{[(2J+1)/(2I+1)]\times[\Gamma_\gamma\Gamma_C/(\Gamma_\gamma+\Gamma_C)]\}-50.4E^*/T, \tag{21}$$

with Γ and E^* in Mev. Here $E^*=E_r+Q$.

If no level is sufficiently close to the separation energy (and above it), we must also consider the nonresonant rate. Because of the energy width assigned to each level, each interval dE^* of the excitation energy range obtains from the neighboring resonances (E_r) a population of

$$p(E^*)dE^*=[(2J+1)/(2I+1)]\Gamma_\gamma\exp(-E^*/KT)dE/\{\Gamma^2/4+[E^*-(E_r+Q)]^2\}. \tag{22}$$

Integrating over a resonance, we would get back Eq. (20).

[8] M. Burbidge *et al.*, Revs. Modern Phys. **29**, 581 (1957).

TABLE I. Possible outcomes of the carbon-carbon reaction at stellar energies, with their respective Q values (in Mev).

Outcome	$Mg^{24}+\gamma$	$Na^{23}+p$	$Mg^{23}+n$	$Ne^{20}+\alpha$	$O^{16}+Be^{8}$	$O^{16}+2\alpha$
Q	13.846	2.230	−2.603	4.619	−0.206	−0.111

The nonresonant rate $\mathcal{P}_{n.r.}^{dis}$ is then given by

$$\mathcal{P}_{n.r.}^{dis}=\int p(E^*)dE^*\Gamma_{dis}(E^*)/\hbar. \quad (23)$$

It is best to express it in terms of the probability of the photocapture $\mathcal{P}^{cap}$; we have

$$\log\mathcal{P}^{dis}=\log\mathcal{P}^{cap}+32.28+(\tfrac{3}{2})\log T -\log[(2I+1)/(2j_1+1)(2j_2+1)] +(\tfrac{3}{2})\log A-50.4Q/T, \quad (24)$$

Q is the energy released during the photocapture.

The qualitative arguments given here have a simple statistical mechanical justification; Eq. (24) is merely a statement of the law of mass action.

3. REACTION $C^{12}-C^{12}$

The possible outcomes of the collision of two carbons at stellar energies are given in Table I. The first four processes are expected to go via compound nucleus formation while the last two involve the so-called exchange reactions.[9] For both kinds of reactions, computations of reaction rates is difficult because of uncertainties in selecting the correct effective radius of interaction.

We consider first the reactions via a compound nucleus C*. If A, B, C, D are light nuclei and e is a proton, neutron, or alpha particle, then the compound nucleus formalism asserts that the cross section for the reaction $A+B\rightarrow D+e$ is

$$\sigma(A+B\rightarrow D+e)=\sigma(A+B\rightarrow C^*)P(C^*\rightarrow D+e),$$

where the first factor on the right-hand side is the cross section for formation of the compound nucleus C^* and the second factor P is the branching ratio for the decay of the compound nucleus into the particular channel $D+e$. For calculating $\sigma(A+B\rightarrow C^*)$ we shall use the "black-nucleus" picture discussed in Sec. 2a, so the only unknown parameter is the effective interaction radius R. This cross section has a "knee" at kinetic energies close to the Coulomb barrier for this radius and well below this knee the cross section decreases very rapidly with decreasing energy and depends extremely sensitively on the numerical value of R. For our $C^{12}+C^{12}$ reaction the relevant kinetic energies are about 1 or 2 Mev, very far below the knee indeed.

Since no direct experiments on our reaction are available, we attempt to obtain values for R from cross-section measurements for other reactions $A+B\rightarrow D+e$ via a compound nuclei C^* close in mass to Mg^{24}. Two methods are available in principle: (1) If the cross section has been measured at incident energies appreciably below the Coulomb barrier, the calculated value for $\sigma(A+B\rightarrow C^*)$ depends strongly on the assumed value for R. If we can estimate the branching ratio $P(C^*\rightarrow D+e)$ we can then find the value of R for which the calculated cross section $\sigma(A+B\rightarrow C+D)$ agrees with the experimental one. (2) The energy position of the "knee" of the cross-section curve and its logarithmic derivative depend on the value of R. The branching ratios P should be much less energy sensitive than the cross section below the knee and one can compare the logarithmic derivatives of the theoretical $\sigma(A+B\rightarrow C^*)$ for various assumed values of R with that of the experimental $\sigma(A+B\rightarrow D+e)$ at energies below and near the knee. This should give another estimate for R independent of any value assumed for P (except for assuming it to be constant).

Unfortunately the experiments available to date do not extend to adequately low energies. We nevertheless have carried out rough analyses of this type on three different experiments. The first one,[10] on $Li^6+Li^7\rightarrow p+B^{12}$, was rather hard to interpret along these lines. However, it favored a rather large R (at least 8 fermis). The second one, $B^{11}+N^{14}\rightarrow p+Na^{24}$, yielded a radius of about 8.6 fermis.[11] Such a radius gives fairly similar curvatures to the logarithmic derivatives, as can be seen in Fig. 1. Because in this case proton emission has to compete very unfavorably with neutron and alpha emission, its branching ratio is expected to be small and hard to determine. The radius chosen here implies a proton branching ratio of less than 1%, probably an underestimate.

The third[12] reaction is $C^{12}+N^{14}\rightarrow Na^{22}+\alpha$. Here the low-energy data are missing, and we are almost above

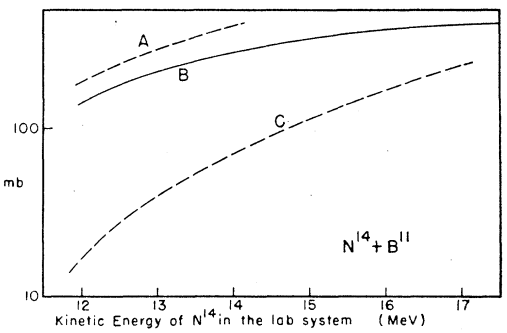

FIG. 1. B is the experimental cross section for the reaction $N^{14}+B^{11}\rightarrow Na^{24}+p$, multiplied by one hundred. A and C are theoretical estimates of the cross section for the reaction $N^{14}+B^{11}\rightarrow Mg^{25*}$, using a radius of interaction of 8.6 and 6.7 fermis, respectively. A logarithmic scale is used to allow direct comparison of the logarithmic derivatives.

[9] The possible importance of this kind of reaction was pointed out to us by A. G. W. Cameron (private communication).

[10] E. Norbeck, Jr., and C. S. Littlejohn, Phys. Rev. **108**, 754 (1957).

[11] H. L. Reynolds *et al.*, Phys. Rev. **102**, 237 (1956).

[12] H. L. Reynolds *et al.*, Phys. Rev. **96**, 1615 (1954).

the "knee" of the Coulomb curve. The absolute value of the cross section and the logarithmic derivatives are pretty well in agreement and give a radius of roughly 6.4.

Two remarks about these radii. First, they are surprisingly large. The usual formula $R=1.25(A_1^{\frac{1}{3}}+A_2^{\frac{1}{3}})$ would not have predicted radii bigger than 6 fermis. A different approach used by Hayashi *el at.* and by Cameron[5] had yielded equally large radii. Second, the radii seem to vary rather strongly for neighboring nuclei. However, comparing $B^{11}+N^{14}$ with $C^{12}+N^{14}$, it is probably reasonable, in view of the compactness of C^{12} compared to B^{11}, to find for this last pair a smaller radius of interaction.

To use these results in our work, we have assumed that the radius is independent of the incident energy. Allowing for the uncertainties and the observed variations, we use

$$\begin{aligned} R_<&=1.25(A_1^{\frac{1}{3}}+A_2^{\frac{1}{3}})+0.8 \text{ (fermis), (lower limit)} \\ R_>&=1.25(A_1^{\frac{1}{3}}+A_2^{\frac{1}{3}})+2.9 \text{ (fermis), upper limit)} \end{aligned} \tag{25}$$

where A_1 and A_2 are the masses of the two colliding nuclei.

For the $C^{12}+C^{12}$ reaction, this formula assigns a smaller radius ($R_<$) of 6.5 fermis, and a larger radius ($R_>$) of 8.6 fermis. These values should give a lower and an upper limit to the rate. However, because of the compactness of the carbon nuclei, the smaller radius is probably more nearly correct.

The "black" nucleus formalism was used for the computation of the rate. The factor n [see Eq. (16)] was estimated to be about 0.05. We obtain $S_{b<}'=5.5\times10^{17}$ ev barns and $S_{b>}'=2.1\times10^{20}$ ev barns. The rates are given by

$$\begin{aligned} \mathcal{P}_<&=(3.0\times10^3)[10^{-[(78.74/T^{\frac{1}{3}})(1+2.4\times10^{-3}T)]}]/T^{\frac{3}{2}}, \\ \mathcal{P}_>&=(1.1\times10^6)[10^{-[(78.74/T^{\frac{1}{3}})(1+3.6\times10^{-3}T]}]/T^{\frac{3}{2}}. \end{aligned} \tag{26}$$

In Table II and in Fig. 2, the rate and the lifetime of C^{12} as a function of the temperature are given for a density of 10^4 g/cc.

We want now to discuss the decay of the compound nucleus (C.N.), i.e., evaluate the branching ratios of various possible outcomes.

The neutron emission is treated first. An upper limit to the branching ratio (C.N.) can be obtained by assuming that every collision which involves more than the threshold energy (E_t) will result in neutron emission. This upper limit to the branching ratio, obtained numerically as the integral of the reaction rate from E_t to ∞ divided by the integral from 0 to ∞, is 2×10^{-4}, 10^{-2}, and 5×10^{-2}, respectively, for $T=6$, 8, and 10. In reality the neutron partial widths are very small except for C.N. states leading to s-wave neutrons (about one third of all states) and even for s-waves they are small and proportional to $E_n^{\frac{1}{2}}$ for neutron energies E_n less than about 0.1 Mev. A numerical calculation gave, as a more reasonable estimate[13] for the neutron branching ratios: 3×10^{-5}, 2×10^{-3}, and 1×10^{-2}, respectively, for $T=6$, 8, and 10.

For emission of protons, alpha particles and Gamma rays, we could in principle use the experimental[14] evidence on $Na^{23}+p$. Baumann *et al.*[14] have studied this reaction in an energy range from 12 to 13 Mev excitation energy. From analysis of their work, we can, by extrapolation, obtain the following rough information: at 15 Mev the proton branching ratios are about 0.75, 0.25, and 0.01 for protons, alphas, and gammas, respectively.

However, Friedman and Weisskopf[15] point out that

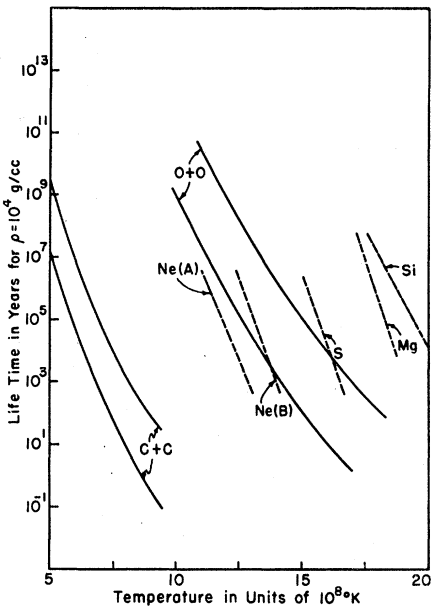

FIG. 2. The curves (C+C) are, respectively, an upper and a lower limit to the mean life of a C^{12} nucleus in a gas of C^{12}, with $\rho=10^4$ g/cc. The curves (O+O) are the equivalent limits for the case of O^{16}. The shorter curves are the mean life of various nuclei against photodisintegration. Ne(A) is the correct one for Ne^{20}, if the 5.631-Mev level is "active" (see text). If not, Ne(B) is the correct one.

TABLE II. Reaction rates ($\mathcal{P}$) for the heavy-ion processes (in cm^3 sec^{-1}). The $\mathcal{P}_<$ and $\mathcal{P}_>$ are lower and upper limits, respectively. Also given are the mean life in years of one of these ions when the density is 10^4 g/cc.

T	5	6	8	10	15	20
$-\log_{10}\mathcal{P}_<$(C+C)	43.6	41.0	37.3			
$-\log_{10}\mathcal{P}_>$(C+C)	41.4	38.7	35.0			
$\log_{10}t_<$(C+C)	9.4	6.8	3.1			
$\log_{10}t_>$(C+C)	7.1	4.5	0.8			
$+\log_{10}t_<$(O+O)				12.0	5.0	0.8
$+\log_{10}t^>$(O+O)				8.9	2.1	−2.0

[13] Our branching ratio at $T=6$ is considerably smaller than that estimated by F. Hoyle, Suppl. Astrophys. J. **1**, 121 (1954). This discrepancy is largely due to a change in the Q-values brought about by more recent and accurate measurements. The neutron lies about 0.95 Mev above the Gamow peak, compared with Hoyle's estimate of 0.65 Mev.

[14] N. P. Baumann *et al.*, Phys. Rev. **104**, 376 (1956).

[15] F. L. Friedman and V. F. Weisskopf, *Niels Bohr and the Development of Physics* (Pergamon Press, London, 1955), p. 134.

in the region of excitation energy of the C.N. where the levels just start to overlap, the assumption that the decay of the C.N. is independent of its mode of formation is no longer realistic. There is a tendency for the proton emission branching ratio to be enhanced if the reaction is initiated by protons. Coulomb barrier penetration factors and the simple C.N. picture would predict slightly more alpha emission than proton emission. For our work we shall adopt branching ratios of about 0.5, 0.5, and 0.01, respectively, for alpha, proton, and photon emission.

The two next reactions on our list are believed not to involve the formation of a C.N. They can be pictured as a mere rearrangement of the constituents of the nucleus, and such a rearrangement can occur at larger intercenter distance than is needed for a C.N. However, we have estimated that interaction radii of about 12 f or more would be required for these transfer reactions to compete with the first four C.N. reactions. It is unlikely that transfer reactions occur at such large distances and we shall neglect these reactions.[16,17]

4. SUBSEQUENT REACTIONS

As discussed in Sec. 1, we shall restrict ourselves to a temperature range of 6×10^8 to 9×10^8 °K for which there action times for the C−C collision range from about 10^6 years to 1 year.

From the steady output of protons and alphas resulting from the carbon reaction, a complicated series of nuclear reactions will be generated. These particles will first interact with the initial assembly of carbon, oxygen, and neon, and later will start interacting with sodium and various other nuclei generated by these reactions. The final distribution of isotopic abundances will depend very strongly on the temperature involved, i.e., on the time allowed for each reaction. This reaction-time dependence is brought in by the fact that the nucleus N^{13} will in our range of temperature pass by a point where its life against photodisintegration is equal to its life against beta decay; at $T=6\times10^8$ °K, the nucleus will beta decay, while at 8×10^8 °K, it will be photodisintegrated. In the low-T case, a large flux of neutrons is generated through the reaction $C^{13}(\alpha,n)O^{16}$, while in the second case a smaller flux of neutrons will come from $C^{12}+C^{12}\rightarrow Mg^{23}+n$, and from $Ne^{21}(\alpha,n)Mg^{24}$.

The analysis of the situation requires knowledge of the various reaction rates of alphas, protons, and neutrons in the gas constituents. The three following subsections will be devoted to computations of these rates.

TABLE III. The reaction rates per unit pair of particles ($\mathcal{P}$) are listed under the form of $(-\log_{10}\mathcal{P})$, for various temperatures. The units of $\mathcal{P}$ are $cm^3\ sec^{-1}$; the units of temperature are 10^8 °K. For the meaning of (*A*), (*B*), and (*C*) see Sec. 4.

T	5	6	8	10	20
$C^{12}+\alpha-O^{16}+\gamma$	32.9	32.1	30.9	30.0	27.6
$C^{13}+\alpha\rightarrow O^{16}+n$	26.3	25.2	24.1	22.9	
$N^{14}+\alpha\rightarrow F^{18}+\gamma$	27.3	27.1	26.7	26.5	
$N^{15}+\alpha\rightarrow F^{19}+\gamma$	27.3	27.1	26.7	26.5	
$O^{16}+\alpha\rightarrow Ne^{20}+\gamma$ (*A*)	31.1	29.6	27.9	26.9	25.1
$O^{16}+\alpha\rightarrow Ne^{20}+\gamma$ (*B*)	33.9	33.6	32.9	30.5	25.9
$O^{16}+\alpha\rightarrow Ne^{20}+\gamma$ (*C*)	36.8	35.9	32.9	30.5	25.9
$O^{17}+\alpha\rightarrow Ne^{20}+n$	29.0	28.5	26.2	24.9	
$O^{18}+\alpha\rightarrow Ne^{21}+n$	29.0	28.5	26.2	24.9	
$Ne^{20}+\alpha\rightarrow Mg^{24}+\gamma$	29.9	28.6	26.3	24.7	
$Ne^{21}+\alpha\rightarrow Mg^{24}+n$	29.9	28.6	26.3	24.7	
$Na^{23}+\alpha\rightarrow Mg^{26}+p$	30.8	28.9	27.0	25.5	
$Mg^{24}+\alpha\rightarrow Si^{28}+\gamma$	32.0	30.5	27.9	26.4	
$Mg^{25}+\alpha\rightarrow Si^{28}+n$	32.0	30.5	27.9	26.4	
$Mg^{26}+\alpha\rightarrow Si^{29}+n$	32.0	30.5	27.9	26.4	
$Al^{27}+\alpha\rightarrow Si^{30}+p$	32.6	30.9	28.3	26.7	
$Si^{28}+\alpha\rightarrow S^{32}+\gamma$	34.6	32.8	30.4	28.4	
$S^{32}+\alpha\rightarrow A^{36}+\gamma$	36.0	34.9	32.1	29.9	
$A^{36}+\alpha\rightarrow Ca^{40}+\gamma$	38.9	36.8	33.7	31.6	
$Ca^{40}+\alpha\rightarrow Ti^{44}+\gamma$	41.0	38.9	35.3	32.8	
$Ti^{44}+\alpha\rightarrow Cr^{48}+\gamma$	42.8	40.8	36.8	34.3	
$C^{12}+p\rightarrow N^{13}+\gamma$	22.6	22.1	21.3	20.9	
$C^{13}+p\rightarrow N^{14}+\gamma$	22.4	21.7	20.8	20.3	
$N^{14}+p\rightarrow O^{15}+\gamma$	22.7	22.4	22.0	21.8	
$N^{15}+p\rightarrow C^{12}+\alpha$	18.5	18.1	17.6	17.3	
$O^{17}+p\rightarrow N^{14}+\alpha$	20.8	20.1	19.4	18.9	
$O^{18}+p\rightarrow N^{15}+\alpha$	20.5	19.7	18.8	18.4	
$Ne^{20}+p\rightarrow Na^{21}+\gamma$	25.3	24.7	23.9	23.3	
$Ne^{21}+p\rightarrow Na^{22}+\gamma$	26.2	25.6	24.8	24.8	
$Na^{23}+p\rightarrow Ne^{20}+\alpha$	21.9	21.1	20.1	19.6	
$Na^{23}+p\rightarrow Mg^{24}+\gamma$	22.4	22.0	21.3	20.6	
$Mg^{24}+p\rightarrow Al^{25}+\gamma$	22.1	21.8	21.5	21.1	
$Mg^{25}+p\rightarrow Al^{26}+\gamma$	22.5	22.4	21.7	21.0	
b.n. (see text)	21.8	21.3	20.6	19.8	
$Mg^{26}+p\rightarrow Al^{27}+\gamma$	21.3	21.0	20.6	20.2	
$Al^{27}+p\rightarrow Mg^{24}+\alpha$	22.3	21.7	20.7	20.1	
$Al^{27}+p\rightarrow Si^{28}+\gamma$	22.3	21.7	20.7	20.1	
$Si^{28}+p\rightarrow P^{29}+\gamma$	23.0	22.8	22.6	22.6	
$C^{12}+n\rightarrow C^{13}+\gamma$		20.2		20.2	
$C^{13}+n\rightarrow C^{14}+\gamma$		20.0		19.8	
$N^{14}+n\rightarrow N^{15}+\gamma$		18.8		18.8	
$N^{14}+n\rightarrow C^{14}+p$		18.5		18.1	
$N^{15}+n\rightarrow N^{16}+\gamma$		23.3		23.3	
$O^{16}+n\rightarrow O^{17}+\gamma$		21.6		20.7	
$O^{17}+n\rightarrow C^{14}+\alpha$		17.2		16.9	
$O^{18}+n\rightarrow O^{19}+\gamma$		22.4		22.4	
$Ne^{20}+n\rightarrow Ne^{21}+\gamma$		20.5		20.5	
$Ne^{21}+n\rightarrow Ne^{22}+\gamma$		19.2		19.2	
$Ne^{22}+n\rightarrow Ne^{23}+\gamma$		20.2		20.2	
$Na^{23}+n\rightarrow Na^{24}+\gamma$		18.7		18.8	
$Mg^{24}+n\rightarrow Mg^{25}+\gamma$		19.2		19.2	
$Mg^{25}+n\rightarrow Mg^{26}+\gamma$		19.0		19.0	
$Mg^{26}+n\rightarrow Mg^{27}+\gamma$		20.3		20.1	
$Al^{27}+n\rightarrow Al^{28}+\gamma$		18.5		18.6	
$Si^{28}+n\rightarrow Si^{29}+\gamma$		18.6		18.9	

[16] This estimate was obtained in the following way: The expression for the general element of the scattering matrix between two different states [see for instance D. C. Peaslee, *Annual Review of Nuclear Science* (Annual Reviews, Inc., Palo Alto, 1955), Vol. 5, p. 103, Eq. (3)] contains the product of the penetration factors (P) pertaining to the two states. These factors are highly radius dependent. Equating the rate of two processes (C.N. and transfer processes), we obtain the radii quoted.

[17] In the previous discussion we have neglected entirely the electron screening effect on the rate of the $C^{12}+C^{12}$ reaction. For not too high densities the screening is accounted for by ascribing an additional potential U_0 at the center of the nucleus, and by multiplying the reaction rate by $\exp[-U_0/kT]$ [E. E. Salpeter, Australian J. Phys. **7**, 373 (1954)]. For densities less then 4×10^5 g/cc the term $(-U_0/kT)$ is less than 0.50, hence the effect is not very important. At $\rho=10^8$ and 10^{10}, $(-U_0/kT)$ is about 3.0 and 13.0. At higher densities $-U_0$ becomes larger than the Gamow energy and the approximations used in the above-mentioned paper break down. This case has been considered by A. G. W. Cameron (unpublished work).

The experimental parameters quoted were taken, when not otherwise mentioned, from Ajzenberg and Lauritsen[18] and Endt and Braams.[18]

The Q values were obtained with the help of the most recent mass determinations.[19]

Some reactions of special interest have been analyzed in detail. For these, the level scheme in the energy region of interest is given, together with the experimentally measured parameters. E^* is the excitation energy in Mev of a resonance level in the compound nucleus formed; J, π denotes the spin and parity of the level; Γ_γ; etc. are the partial widths. For other reactions, we merely mention the method used. The results are given in Table III.

(1) $C^{12}+\alpha \rightarrow O^{16}+\gamma$; $Q=7.148$ Mev

E^* (Mev)	7.121	8.875	9.58
$J\pi$	1−	2−	1−
Γ_γ (ev)	6.6×10^{-2}		6×10^{-3} [20]

For T less than 15 the main contribution comes from the upper wing of the 7.121-Mev level. Above this temperature, the contribution from the 9.58-Mev level is dominant.

(2) $C^{13}+\alpha \rightarrow O^{17}+\gamma$; $Q=6.348$ Mev
$C^{13}+\alpha \rightarrow O^{16}+n$; $Q=2.202$ Mev

E^* (Mev)	6.87	7.163
$J\pi$	$\frac{1}{2}+$	$\frac{5}{2}-$
θ_α^2		0.50

For the lowest level we choose $\theta_\alpha^2=0.02$. The contributions of the two levels are roughly comparable in the lowest part of the range.

(3) $O^{16}+\alpha \rightarrow Ne^{20}+\gamma$; $Q=4.753$ Mev

E^* (Mev)	4.969 [21]	5.631 [22]	6.745
$J\pi$	1−(2−)		0+
Γ_γ (ev)	$<5\times10^{-3}$ [23]		
Γ_α (Mev)			0.024

Because of the uncertainty in the $J\pi$ of the 4.969-Mev and the 5.631-Mev resonances, we have to draw three pictures of the situation. In the first picture (A) we assume that the level at 5.631 Mev is active. In the second picture (B) the level at 5.631 Mev is inactive but the level at 4.969 is active. In the third picture they are both inactive. As seen in Table III, rather different rates are predicted for these three cases.

For the reactions $Ne^{20}+\alpha$, $Mg^{24}+\alpha$, etc., up to $Ti^{44}+\alpha$, and also for a few others mentioned in Table III, the Gamow peak always contains several resonances. We have used the method appropriate to that case. The experimental information assigns a level density of about 10 active levels per Mev for most of these cases. This was assumed to be true in all cases. The average radiation width (times the statistical factor) ($\omega\Gamma_\gamma$) is about 2 ev for S^{32} and 10 ev for Ca^{40}. We choose 1 ev for Mg^{24}, and slowly increasing values for higher A. We choose $\theta_\alpha^2=0.1$ all the way through.

(4) $C^{12}+p \rightarrow N^{13}+\gamma$; $Q=1.941$ Mev

E^* (Mev)	2.365	3.507
$J\pi$	$\frac{1}{2}+$	$\frac{3}{2}-$
θ_p^2	0.54	0.031
$\omega\Gamma_\gamma$ (ev)	0.67	1.39

In the range of temperature considered here, the rate comes mostly from the resonance at 2.365 Mev.

The half-life of N^{13} against photodisintegration is 3×10^4 seconds at $T=6$; 0.3 second at $T=8$, and 3×10^{-4} second at $T=10$. As we are interested here in the formation of C^{13}, the rate $\mathcal{P}(C^{12}+p \rightarrow N^{13})$ should be multiplied by the ratio $\mathcal{P}(N^{13} \rightarrow C^{13})/[\mathcal{P}(N^{13} \rightarrow C^{13})+\mathcal{P}(N^{13} \rightarrow C^{12}+p)]$ (the half-life of N^{13} against beta decay is 600 sec).

(5) $C^{13}+p \rightarrow N^{14}+\gamma$; $Q=7.546$ Mev

E^* (Mev)	7.962	8.06
$J\pi$		1−
θ_p^2		1.13
$\omega\Gamma_\gamma$ (ev)		8.6

As seen from the table, the value of the radiation width of the 7.962-Mev state would decide which level is more important. We assume $\Gamma_\gamma=0.7$ ev for this level.

(6) $O^{16}+p \rightarrow F^{17}+\gamma$; (7) $Ne^{20}+p \rightarrow Na^{21}+\gamma$

For both the nonresonant contribution dominates. We use the new experimental value of $S=6\times10^{-3}$ Mev barn, and 6×10^{-2} Mev barn, respectively.

In our range of temperature, F^{17} will always be photodisintegrated before it has time to undergo beta decay; Na^{21} will almost always undergo beta decay before it has time to be photodisintegrated.

(8) $Na^{23}+p \rightarrow Mg^{24}+\gamma$; $Q=11.687$ Mev
$Na^{23}+p \rightarrow Ne^{20}+\alpha$; $Q=2.38$ Mev

Because of the importance of these two reactions for our work, and also because of the surprisingly small rates obtained, we give a more detailed discussion of the computations.

Five different papers have been used and checked for consistency; their results are gathered here.[24–28] (See

[18] F. Ajzenberg and T. Lauritsen, *Energy Levels of Light Nuclei VI, Z=1 to 10* (North-Holland Publishing Company, Amsterdam, 1959); P. M. Endt and C. M. Braams, Revs. Modern Phys. **29**, 683 (1957).

[19] A. H. Wapstra, Physica **21**, 378 (1955); **21**, 403 (1955). J. Mattauch *et al.*, *Annual Review of Nuclear Science* (Annual Reviews, Inc., Palo Alto, 1956), Vol. 6, p. 199; T. T. Scolman *et al.*, Phys. Rev. **102**, 1078 (1956); K. S. Quisenberry, Phys. Rev. **107**, 1664 (1957).

[20] Toppel, Bloom, and Wilkinson, Phil. Mag. **2**, 57 (1957).

[21] Recent experiments reinstall the possibility of this level being 2− [T. H. Kruse (private communication)].

[22] This level is observed in the $Ne^{20}(\alpha,\alpha)Ne^{20*}$. It is not a 0−. Statistical arguments make it likely to be an active level.

[23] H. Gove and A. Litherland (private communication).

[24] J. Freeman and A. Baxter, Nature **162**, 696 (1948).

[25] F. C. Flack *et al.*, Proc. Phys. Soc. (London) **A67**, 974 (1954).

[26] P. J. Grant *et al.*, Proc. Phys. Soc. (London) **A68**, 374 (1955).

[27] D. A. Hancock and F. Verdaguer, Proc. Phys. Soc. (London) **A68**, 1080 (1955).

[28] N. P. Baumann and F. Prosser, Phys. Rev. **104**, 376 (1956).

TABLE IV. Resonances of importance in the $Na^{23}+p \rightarrow Mg^{24}+\gamma$ reaction and their characteristics.

E^* (Mev)	$J\pi$	$(2J+1)\Gamma_\alpha$ (ev)	$(2J+1)\Gamma_\gamma$ (ev)
11.928		<0.02?	0.005
11.962		0.2	<0.005
11.983	2−	<0.02	0.4
12.011		0.2	<0.01
12.045		<0.05	0.01
12.111		<0.05	0.02
12.177	1+	<0.05	0.2
12.256	2−, 3−	500	0.4
12.329	3+	<0.2	1.4
12.467	2+	2000	

Table IV.) Some of the $(2J+1)\Gamma_\alpha$ and $(2J+1)\Gamma_\gamma$ were obtained from references 25 and 27 by treating the yields in the manner given by Bethe.[29] Upper limits were found using the sensitivity of the experimental setup in reference 25.[30] The rates given in Table III were obtained by summing the resonant rates over all the levels in Table IV. From the background yields between resonances given in references 24 and 28, one can estimate an upper limit to the nonresonant rate of the (p,α) reaction; at $T=6$ this estimate gave -22.0 for $\log\mathcal{P}$ and the nonresonant contribution is thus unimportant.

As mentioned before, our rates in Table III for $Na^{23}(p,\alpha)$ are surprisingly low and only three times larger than the (p,γ) rate. This is due to the fact that the measured widths are so small for the known levels in the most suitable energy range, $E_r \equiv E^* - 11.68$ Mev ~ 0.4 Mev. For very low proton energies E_r, on the other hand, the Wigner-Teichman upper limit for Γ_p is quite small—about 2 ev for $E_r=0.24$ Mev—so that the combination $(2J+1)\Gamma_p\Gamma_\alpha(\Gamma_p+\Gamma_\alpha)^{-1}$ is then small even if Γ_α is large. Thus the (p,α) rate in Table III would be increased by at most a factor of 20 even if Γ_α were exceedingly large for the level at $E^*=11.928$ (for which Γ_γ is certain but Γ_α somewhat in doubt) or for any hypothetical level at lower energies. Similarly, any such hypothetical level could increase the (p,γ) rate in Table III by at most a factor of 10.

(9) $\mathbf{Mg^{24}+p \rightarrow Al^{25}+\gamma;\ Q=2.29\ Mev}$

E^* (Mev	2.51	2.69
$J\pi$	$\frac{1}{2}+$	$\frac{3}{2}+$
Γ_γ (ev)	0.014 [31]	0.014

Most of the contribution comes from the lowest level.

(10) $\mathbf{Mg^{25}+p \rightarrow Al^{26}+\gamma;\ Mg^{26}+p \rightarrow Al^{27}+\gamma}$

As excellent experimental information was available on these experiments, a detailed calculation was made taking into account 13 levels in the first case and 5 in the second, and the reaction rate thus obtained was compared with the prediction of the "black" nucleus formalism. Good agreement was found.

The reactions $N^{14}+p \rightarrow O^{15}+\gamma$, $N^{15}+p \rightarrow C^{12}+\alpha$, $O^{17}+p \rightarrow N^{14}+\alpha$, $O^{18}+p \rightarrow N^{15}+\alpha$, $Al^{27}+p \rightarrow Mg^{24}+\alpha$, and $Si^{28}+p \rightarrow P^{29}+\gamma$ were all found to be resonant with at most one or two resonances within the Gamow peak.

(11) $\mathbf{C^{12}+n \rightarrow C^{13}+\gamma;\ Q=4.946\ Mev}$

The cross section at thermal energy is 3.3 mb. It decreases with energy more slowly than the typical $1/v$ law. The resonant rate is negligible. $\mathrm{Log}\mathcal{P}_{n.r.} = -20.2$ (all through the range $6 \leqslant T \leqslant 10$).

(12) $\mathbf{C^{13}+n \rightarrow C^{14}+\gamma;\ Q=8.174\ Mev}$

There is one resonance at $E_n=0.146$ Mev. We assume for it $\Gamma_\gamma=0.3$ ev and get $\log\mathcal{P}_r=-20.0$ $(6 \leqslant T \leqslant 10)$. The thermal cross section is 0.7 mb; $\log\mathcal{P}_{n.r.}=-20.9$.

(13) $\mathbf{N^{14}+n \rightarrow N^{15}+\gamma;\ Q=10.842\ Mev}$
$\mathbf{N^{14}+n \rightarrow C^{14}+p;\ Q=0.678\ Mev}$

E^* (Mev)	11.299	11.438	11.61
$J\pi$	$\frac{1}{2}-$	$\frac{1}{2}+$	$\frac{1}{2}+$
$\omega\Gamma_n\Gamma_\gamma/\Gamma$ (ev)	1.25×10^{-2}	0.56	0.1
$\omega\Gamma_n\Gamma_p/\Gamma$ (ev)	460	2200	1600

The $(\omega\Gamma_n\Gamma_\gamma/\Gamma)$ and $(\omega\Gamma_n\Gamma_p/\Gamma)$ were obtained from Bartholomew *et al.*[32] The thermal cross section is 1.75 b for (n,p) and 80 mb for (n,γ).

(14) $\mathbf{O^{16}+n \rightarrow O^{17}+\gamma;\ Q=4.146\ Mev}$

The thermal cross section is less than 0.2 mb. A resonance at $E_n=0.433$ Mev (lab) accepts $l=1$ neutrons. We assume that $\Gamma_\gamma=0.5$ ev.

(15) $\mathbf{O^{17}+n \rightarrow O^{18}+\gamma;\ Q=8.069\ Mev}$
$\mathbf{O^{17}+n \rightarrow C^{14}+\alpha;\ Q=1.826\ Mev}$

The resonance at $E=8.30$ Mev is the main contributor: $\log\mathcal{P}(n,\alpha)=-17.2$.

(16) $\mathbf{Ne^{20}+n \rightarrow Ne^{21}+\gamma;\ Ne^{21}+n \rightarrow Ne^{22}+\gamma;}$
$\mathbf{Ne^{22}+n \rightarrow Ne^{23}+\gamma}$

The nonresonant contributions were estimated to be roughly -20.5, -19.2, and -20.2, respectively.

(17) $\mathbf{Na^{23}+n \rightarrow Na^{24}+\gamma;\ Q=6.956\ Mev}$

E^* (Mev)	6.96	7.01
$J\pi$	1+	2−
Γ_γ (ev)	$\leqslant 0.34$ [33]	

In our range of temperatures, the nonresonant contribution and the resonant contributions from the

[29] H. A. Bethe, Revs. Modern Phys. **9**, 207 (1937).
[30] J. G. Rutherglen (private communication).
[31] C. Vander Leun, thesis, University of Utrecht, 1958 (unpublished). This work also contains information about (p,γ) reactions on Mg, Si, P, and S.
[32] G. A. Bartholomew *et al.*, Can. J. Phys. **33**, 452 (1955).
[33] Determined by Lyan, Firk, and Moxon, Nuclear Phys. **5**, 603 (1958). The authors give good reason why this upper limit should be close to the real value.

two quoted levels are roughly comparable: $\log\wp = -18.7 (6 \leqq T \leqq 10)$.

The reactions $Mg^{24}+n \rightarrow Mg^{25}+\gamma$, $Mg^{25}+n \rightarrow Mg^{26}+\gamma$, $Al^{27}+n \rightarrow Al^{28}+\gamma$, and $Si^{28}+n \rightarrow Si^{29}+\gamma$ all get most of the contribution to their rates through one resonance. For $Mg^{26}+n \rightarrow Mg^{27}+\gamma$, the nonresonant rate seems dominant.

We shall also need neutron absorption cross sections for all the stable isotopes which can be built up by neutron absorptions and beta-decays on a slow time-scale, starting from Fe^{56}. These cross sections are needed for neutron energies of about 60 kev and have been estimated previously for each isotope by Cameron.[5,34]

5. THE ISOTOPIC ABUNDANCES

In Sec. 3 we have calculated the rates at which alpha particles, protons, and neutrons are produced and C^{12} destroyed by the C−C reactions and in Sec. 4 the rates at which alphas, protons, and neutrons are absorbed by various isotopes (Table III). Using these rates one can set up a set of simultaneous differential equations which relate the time derivative of the concentration of each isotope to the actual concentration of various isotopes. These equations were solved numerically, partly with the help of an IBM-650 computer at Cornell.

The solutions depend in principle on the temperature, density and initial composition of the gas. Calculations were carried out for two different temperatures, $T=6$ and 8.5 ($\times 10^8$ °K), for a density of 10^4 g/cc. The corresponding reaction times (see Table II) are of the order of 10^6 years and 10 years, respectively. The results at these two temperatures differ considerably from each other, but the variation inside each of the two ranges $T=5$ to 7 and $T=8$ to 9 is relatively small and changes in density of a factor of 100 have little effect on the final abundances. Some of the calculations were carried out for an initial composition of equal numbers of C^{12}, O^{16}, and Ne^{20}. We shall express the increase in the abundance of an isotope as number of nuclei per number of C^{12} nuclei present originally. Expressed in this form, the results were found to be rather insensitive to variations in the amounts of O^{16} and Ne^{20} present originally. Since the medium and heavy elements are good neutron absorbers, the results are sensitive to the abundance of elements in the Fe region present originally and calculations were carried out for two values of this abundance. We assume throughout that the ratio of alphas to protons produced by C+C is unity. Variations by a factor of three in this ratio do not alter the results very strongly. The results are summarized in Table V.

TABLE V. Stellar gas composition at the end of the $C^{12}-C^{12}$ reaction, at $T=6\times10^8$ and $T=8.5\times10^8$ °K. The abundances of the light elements ($A<30$) are given as a fraction of the original number of C^{12} nuclei. ΔO^{16} means the increase in the abundance of O^{16} nuclei.

T	ΔO^{16}	ΔNe^{20}	Na^{23}	Mg^{24}	Mg^{25}	Mg^{26}	Al^{27}	Si^{28}	Si^{29}
6	0.12	0.14	0.08	0.17	0.024	0.010	0.008	0.003	7×10^{-5}
8.5	0.06	0.06	0.06	0.28	0.02	0.01	0.004	0.002	2×10^{-5}

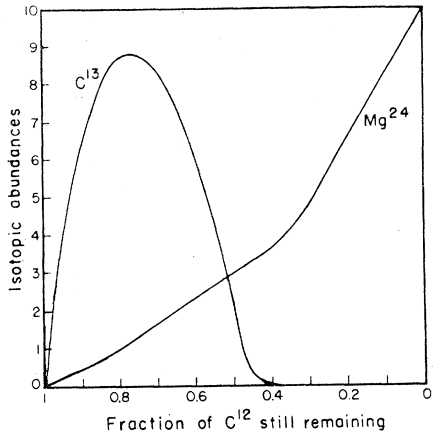

FIG. 3. Time variation of the abundances of various isotopes during the carbon burning. The concentration of C^{13} (relative to initial C^{12} concentration) has been multiplied by 500, the concentration of Mg^{24} by 70.

(a) $T=6\times10^8$ °K

At this temperature the amount of direct neutron production from C+C collisions is negligible, but neutrons are formed indirectly as follows: A reasonable fraction of the protons produced are absorbed by C^{12} and the resulting N^{13} undergoes beta decay to C^{13} with little competition from photodisintegration at this temperature. This is followed by $C^{13}(\alpha,n)O^{16}$, the alpha-absorption rate of C^{13} being a few thousand times larger per nucleus than that of any other isotope present in the gas.

We consider first the case in which no metals are present At least at the early stages of development the main absorber of neutrons is C^{12}, giving C^{13}, followed again by $C^{13}(\alpha,n)O^{16}$, etc. Effectively the C^{13} and the neutrons act merely as catalysts for the conversion of C^{12} plus alphas into O^{16}. In spite of the large $C^{13}(\alpha,n)$ rate, the C^{13} concentration is surprisingly large until about half the original C^{12} is exhausted. As shown in Fig. 3 (which also contains the time variation of Mg^{24}), the C^{13} concentration reaches a maximum of about 0.01 (by number, relative to the original concentration

[34] *Note added in proof.*—More recently R. Macklin *et al.* (unpublished) have measured cross sections in this energy range for a number of elements (averaged over the naturally occurring isotopic abundances). In a number of cases the measured values are somewhat lower than the previous estimates[5] and we have attempted to revise Cameron's estimates[5] for the cross sections σ for each individual isotope in the light of these measurements. We need the sum of σ^{-1} for successive neutron absorptions, starting from Fe^{56}. Expressed in units of $(mb)^{-1}$ this sum up to Zn^{68}, Rb^{85}, Zr^{92}, and Ce^{140} is, respectively, about 1.7, 1.9, 2.6, and 3.2. All numerical results in the remainder of this paper have been altered accordingly.

of C^{12}) and then decreases very sharply to less than 10^{-5} when enough other neutron absorbers (e.g., Na^{23}, Mg^{24}) have been built up.

The neutron concentration is also relatively large at the early stages, about 3×10^{-21}, drops slowly by a factor of about 6 during the first half of the C^{12} burning, and drops very rapidly by another factor of about 3 when the C^{13} concentration drops sharply. In the second half, the neutron concentration decreases roughly as the cube of the C^{12} concentration. The alpha-particle concentration is relatively low (about 10^{-14}) while C^{13} is abundant, increases sharply to about 10^{-12} when C^{13} becomes rare and then decreases slowly in the second half of C^{12} burning. The proton concentration is about 5×10^{-19} in the beginning and decreases slowly, roughly as the square of the C^{12} concentration.

In principle, reaction cycles analogous to $C^{12}(p,\gamma)N^{13}\rightarrow C^{13}$, $C^{13}(\alpha,n)O^{16}$, and $C^{12}(n,\gamma)C^{13}$ are possible with O^{16} or Ne^{20} taking the place of C^{12}. In practice, however, these cycles are much less important at $T=6$ since F^{17} is photodisintegrated instead of undergoing beta decay and Ne^{20} has a small proton absorption cross section (also O^{16} and Ne^{20} are relatively poor neutron absorbers).

Ne^{20} and Na^{23} are built up directly in the C+C reaction. Mg^{24} is subsequently built up and Na^{23} partially depleted by reactions such as $Na^{23}(p,\gamma)Mg^{24}$, $Na^{23}(p,\alpha)Ne^{20}$, and $Ne^{20}(\alpha,\gamma)Mg^{24}$. Because of the surprisingly small cross section for $Na^{23}(p,\alpha)$ in Table III, the depletion of Na^{23} is not very drastic and the final abundance (Table V) of Na^{23} is not much less than that of Mg^{24}. We have repeated the solutions of the equations assuming a rate for $Na^{23}(p,\alpha)Ne^{20}$ ten times larger than that in Table III (almost an upper limit for this rate): The final Na^{23} abundance was smaller than that in Table V by only a factor of two, the Mg^{24} abundance was increased by a factor of less than 1.5 and the other abundances in Table V were not altered strongly.

The protons and neutrons present in the gas are partly absorbed by Mg^{24}, then by the Mg^{25} thus produced and so on. This absorption chain forms monotonically decreasing amounts of the stable isotopes of Mg, Al, Si, P, S, etc. The proton absorption cross section of Si^{28} is rather small and the final abundances of Si^{29} and heavier nuclei are very small. The absorption chain is not interrupted appreciably by $Mg^{25}(\alpha,n)$ since the rate for this reaction is rather small. Since the concentration of alphas and the cross sections for $Mg^{24}(\alpha,\gamma)$ and $Si^{28}(\alpha,\gamma)$ are relatively small, the final abundances of Si^{28} and S^{32} are not enhanced relative to neighboring nuclei.

We considered next the effect of having small amounts of the "metals in the Fe group" ($50\leqslant A\leqslant 66$) present in the original gas mixture. If the original concentration (by number, relative to C^{12}) of this group is less than 10^{-3}, it has a reasonably small effect on the neutron concentration as a function of time, and hence on the final abundances of all the elements lighter than these metals. On the other hand, the neutron concentrations are relatively large, the "Fe group" and the heavier elements are good neutron absorbers and the original nuclei in the "Fe group" are rapidly processed by neutron absorption into somewhat heavier elements.

In this paper we do not attempt to calculate isotopic abundances of the heavier elements produced in any detail, but only the average number of neutrons absorber per original nucleus in the "Fe group." For this purpose we pretend that the original "Fe group" consisted purely of Fe^{56} and use the "hydrodynamic" approximation[35] for describing the "flow" of nuclei from Fe^{56} to larger atomic weights A. In this approximation the average A to which the iron is processed is found by requiring that the sum of the inverses of the neutron absorption cross sections σ from Fe^{56} to A be equal to the time-integrated neutron flux (in suitable units). Using the estimates for $\sum\sigma^{-1}$ described in Sec. 4, we find that the Fe^{56} should be processed to somewhere in the vicinity of Sr^{88}, i.e., an average of about 30 neutrons absorbed per original Fe nucleus. This value of about 30 neutrons is not very accurate; if, for instance, the integrated neutron flux were lowered by 15% only about 15 neutrons would be absorbed.

Throughout the whole C+C burning an average of about one neutron is produced for ten original C^{12} nuclei. This is a rather copious supply of neutrons so that even if as much as one Fe-nucleus per 1000 C^{12} nuclei were present[36] originally, the neutron flux would not be depressed strongly. For this concentration we find, according to a very rough estimate, about 20 neutrons absorbed per Fe-nucleus; i.e., about 20% of all the neutrons produced are absorbed by iron and the subsequent heavier elements.

(b) $T=8.5\times10^8$ °K

The main difference between this case and the previous one at $T=6$ is due to the fact that N^{13}, formed by $C^{12}(p,\gamma)$, is overwhelmingly photodisintegrated instead of undergoing beta decay, at this higher temperature. As a result C^{12} is not an effective proton absorber and cannot act as a proton-neutron converter through the sequence $C^{12}(p,\gamma)N^{13}(\beta^+)C^{13}(\alpha,n)O^{16}$ as it did in the previous case.

At the early stages of the processes, with C^{12} ineffective and before other proton absorbers have been built up, the proton concentration is relatively very large (7×10^{-16}). Thus some Ne^{21} is made by $Ne^{20}(p,\gamma)$, despite the smallness of the cross section for this reaction, which eventually leads to neutron production via $Ne^{21}(\alpha,n)Mg^{24}$. At this higher temperature there is

[35] E. M. Burbidge *et al.*, Revs. Modern Phys. **29**, 547 (1957).

[36] I.e., about 0.4% by weight of Fe or about one Fe-nucleus per 3×10^4 H-atom in the original hydrogen gas from which the C^{12}, O^{16} and Ne^{20} were formed at a lower temperature.

also a small but non-negligible amount of neutrons produced directly by means of $C^{12}+C^{12} \rightarrow Mg^{23}+n$. Despite these two neutron sources, the neutron production is much smaller at this higher temperature, about 0.005 neutron per original C^{12} nucleus (compared with 0.12 at $T=6$).

Due to the increased proton concentrations, the Na^{23} produced by the C+C reaction is depleted more and Mg^{24} built up more than at $T=6$. The abundances of Mg^{25} to Si^{29} are not altered strongly as Table V shows. If the original gas contained about one Fe nucleus (or less) per 1000 C^{12} nuclei, the neutron flux would be essentially unaltered. Only about two or three neutrons are absorbed by each Fe nucleus.

6. FURTHER REACTIONS

As mentioned in the early parts of this paper, we have assumed for the hypothetical star the following pattern of activity: the stellar core, once depleted of a particular element which it was up to that point using as a fuel, slowly increases its temperature (by gravitational contraction) up to the point where some new nuclear processes go on at an appreciable rate. The energy released from these reactions will stop the gravitational contraction, and hence the temperature stops increasing. The core will proceed to burn this new fuel till its exhaustion, etc.

We have left out entirely any violent processes such as those occurring in supernovae.

From the same point of view we sketch briefly the developments subsequent to carbon burning in this section.

The rates of the (C+N), (C+O), (O+O), (O+Ne) reactions were calculated in a manner similar to the (C+C), using for the radius R the recipe given in Eq. (25). The rate of (O+O) is given in Table II.

After most of the C^{12} has burned out (less than 0.1% of the original concentration remaining), the (C+N) and (C+O) reactions will set in to assist the exhaustion of the carbon. They will produce small amounts of magnesium. This whole process should be over when the star reaches $T=10\times10^8$ °K and has little effect on the abundances.

Then the Ne^{20} will start to be photodisintegrated into $O^{16}+\alpha$ and will do so at a non-negligible rate (half-life of 10^5 years) around 12×10^8 °K. The rate of photodisintegration is plotted in Fig. 2 as a function of T. Curve A is valid if the 5.631-Mev level is active, curve B if it is not active. The alpha particles released by the photodisintegration of Ne^{20} will eventually be absorbed by some of the isotopes present, mainly by Ne^{20}, Na^{23}, and Mg. The net effect is the destruction of Ne^{20} and the buildup of O^{16}, Mg, Al, and Si (plus smaller amounts of S^{32}, etc.).

Near $T=14\times10^8$ °K the $O^{16}+O^{16}$ reactions will begin to be appreciable (see Fig. 2). These reactions result in ($Si^{28}+\alpha$), ($S^{31}+n$), and ($P^{31}+p$) with roughly equal branching ratios. The alpha particles, protons, and neutrons released will undergo a complicated network of reactions similar to those following the $C^{12}+C^{12}$ reaction, but resulting in somewhat heavier nuclei, both because Ne^{20} and lighter elements are now depleted and because of the higher temperatures. Any metals present again act as efficient absorbers for the neutrons.

At slightly higher temperature ($T=16$) the S^{32} will be photodisintegrated to Si^{28} in analogy to the Ne^{20} disintegration at lower temperature. Build-up of nuclei in the Fe region will become possible only at temperatures of about 20×10^8 °K or higher when Mg^{24} and Si^{28} can also be photodisintegrated to O^{16}, followed by $O^{16}+O^{16}$ and further photodisintegrations. The net effect of this cycling is the complete breakup of these nuclei with a copius release of alphas, protons, and neutrons which can then build up the most stable nuclei near Fe.

Details of the reactions outlined in this section will be given in a forthcoming paper.

7. DISCUSSION

The carbon-burning reactions we have discussed in this paper may be of interest from the point of view of energy production in some types of stars. The rate of energy production can be obtained from the lifetimes in Table II plus the fact that the net energy release from carbon burning plus the subsequent network of reactions is about 0.5 Mev per nucleon of the original C^{12}. This compares with about 7 Mev and 1 Mev for hydrogen and helium burning, respectively, at lower temperatures.

We conclude by discussing the significance of the carbon burning reactions for nucleogenesis in stars. Perhaps the most interesting feature is the production of heavy elements from the cosmically very abundant elements around Fe by neutron absorption on a slow (or intermediate) time scale. Other sources[35] for neutrons on a slow time scale operate at a lower temperature where neutron cross sections of the metals are even larger and should be capable of processing metals into much heavier isotopes. The carbon burning source results in the absorption of only about 30 neutrons per "Fe nucleus" (with a great uncertainty in the numerical value) at temperatures below about 7×10^8 °K. On the other hand it is a very copious neutron source in the sense that it is not quenched appreciably even when as much as one "Fe nucleus" was present originally per 1000 C^{12} nuclei. It is interesting to note that Burbidge *et al.*[35] concluded from cosmic isotopic abundances (and their Fig. VI, 3) that neutron sources capable of processing the iron-group metals up to atomic weight about 100 must have been more common than sources capable of producing the really heavy elements.

The elements up to Ne are produced by hydrogen and helium burning at temperatures below 1.5×10^8 °K

and the elements in the Fe peak need temperatures well above 2×10^9 °K for their formation. It is reasonable to suppose that the elements Na to Ca are produced at intermediate temperatures. We have shown that the carbon burning reactions at temperatures between 5×10^8 and 10×10^8 °K produce large amounts of Na^{23} and of the Mg isotopes plus decreasing amounts of Al^{27} and Si, but very little of heavier nuclei. One striking feature of our results is the relatively large ratio of Na^{23} to Mg^{24} produced, 1:2 to 1:5 depending on temperature, compared with the Suess-Urey[37] "cosmic abundance" ratio of 1:15. Our ratio of Mg^{24}:Si^{28} of about 50:1 is also in contrast with the cosmic abundance ratio of 1:1. As outlined in Sec. 6, O^{16} burning and Ne^{20} photodisintegration will take place at slightly higher temperatures and result in the buildup of Si and heavier elements and, indirectly, in the depletion of Na^{23}. We hope to obtain detailed results for these reactions soon. At the moment we can only conclude that carbon burning produces plenty of sodium and magnesium.

[37] See also A. G. W. Cameron (to be published).

ACKNOWLEDGMENTS

We are indebted to Dr. A. G. W. Cameron for many discussions and comments and to Dr. W. A. Fowler, Dr. J. H. Gibbons, Dr. T. H. Kruse, and Dr. J. G. Rutherglen for interesting communications. We want to thank Mr. W. A. Cartledge for a careful checking of the manuscript.

PHYSICAL REVIEW VOLUME 116, NUMBER 6 DECEMBER 15, 1959

Total Neutron Cross Section of Xenon and Krypton*†

D. P. MANN‡ AND W. W. WATSON, *Yale University, New Haven, Connecticut*

AND

R. E. CHRIEN, R. L. ZIMMERMAN,§ AND R. B. SCHWARTZ,|| *Brookhaven National Laboratory, Upton, New York*

(Received July 6, 1959)

By the thermal diffusion method, using 12 meters of hot-wire columns, concentrations of the xenon isotopes in good quantity (about 57% Xe^{129} in the light fraction and 27% Xe^{136} in the heavy one) have been produced without recycling. A fair-sized sample of "light" krypton, analyzing better than 50% Kr^{80}, was available from earlier thermal diffusion separation with recycling by Blais and Watson. These samples together with the normal gases were concentrated to thicknesses of about 3.3 g/cm² in special gas target holders for use with the Brookhaven fast chopper. For krypton, neutron widths and isotopic identifications have been determined for the following levels: 27.9 ev in Kr^{83}, 39.8 ev in Kr^{82}, 106 ev in Kr^{80}, 233 ev in Kr^{83}, 519 ev in Kr^{84}, 580 ev in Kr^{84}, and 640 ev in either Kr^{78} or Kr^{80}. Total widths and radiation widths have been obtained for the 27.9- and 106-ev levels by thick-thin area analysis. For xenon, new resonances are observed at 5.2 ev in Xe^{124}, 9.5 ev in Xe^{129}, 14.1, 46.0, and 76.0 ev all in Xe^{131}, 92.0 ev in Xe^{129}, and 126 ev to be assigned to either the 128, 129, or 130 isotope.

INTRODUCTION

ALTHOUGH measurements on the total slow-neutron cross section of xenon[1] and krypton[2] had already been made, it was clear that, with the combination of the higher resolution of the Brookhaven fast chopper and time-of-flight apparatus and gas samples with good isotopic enrichments, these results could be improved. Since krypton has six isotopes and xenon has nine, it was obviously desirable to have usable amounts of these gases with the normal isotope abundance ratios sufficiently changed to make possible the isotopic identification of each of the resonances. For this purpose it was only necessary to have gas samples of a few hundred cm³ in size and with isotope abundances changed by a factor of two or so. The thermal diffusion method, using hot-wire columns, is the preferred way to accomplish such isotope enrichments in these gases.

A difficulty to be overcome was the concentration of these gases into suitable holders that would go into the small, precisely limited, target area traversed by the collimated neutron beam in the Brookhaven fast chopper entrance stator. This was accomplished by freezing the gas within the proper pressure-temperature range into especially designed Armco iron holders to give sample thicknesses of about 3.3 g/cm².

PRODUCTION OF THE ENRICHED XENON AND KRYPTON SAMPLES

The thermal diffusion apparatus consisted of four, hot-wire, glass columns, each three meters in length, the

* A portion of this material is contained in the dissertation of D. P. Mann, submitted in partial fulfillment of the requirements for the degree of Doctor of Philosophy in Yale University.

† Supported in part by the U. S. Atomic Energy Commission.

‡ Present address: Centre d'Etudes Nucléaires, Saclay, France.

§ Present address: Atomic Energy of Canada Limited, Chalk River, Ontario, Canada.

|| Present address: Atomic Energy Research Establishment, Harwell, England.

[1] S. P. Harris, Phys. Rev. **89**, 904(A) (1953).

[2] S. J. Cocking, J. Nuclear Energy **6**, 113 (1957).